Am J Physiol Heart Circ Physiol 287: H1115–H1124, 2004.
First published May 13, 2004; 10.1152/ajpheart.00075.2004.

Evidence of nanobacterial-like structures in calcified human arteries and cardiac valves

Virginia M. Miller,[1,2] George Rodgers,[6] Jon A. Charlesworth,[3] Brenda Kirkland,[7] Sandra R. Severson,[1] Todd E. Rasmussen,[1] Marineh Yagubyan,[1] Jeri C. Rodgers,[7] Franklin R. Cockerill, III,[4] Robert L. Folk,[7] Ewa Rzewuska-Lech,[1] Vivek Kumar,[5] Gerard Farell-Baril,[5] and John C. Lieske[5]

Departments of [1]Surgery, [2]Physiology and Bioengineering, [3]Biochemistry and Molecular Biology, [4]Clinical Microbiology, and [5]Internal Medicine, Division of Nephrology, Mayo Clinic, Rochester, Minnesota 55905; and [6]Heart Hospital of Austin and [7]Department of Geological Sciences, The University Texas at Austin, Austin, Texas 78712

Submitted 28 January 2004; accepted in final form 11 May 2004

Miller, Virginia M., George Rodgers, Jon A. Charlesworth, Brenda Kirkland, Sandra R. Severson, Todd E. Rasmussen, Marineh Yagubyan, Jeri C. Rodgers, Franklin R. Cockerill III, Robert L. Folk, Ewa Rzewuska-Lech, Vivek Kumar, Gerard Farell-Baril, and John C. Lieske. Evidence of nanobacterial-like structures in calcified human arteries and cardiac valves. *Am J Physiol Heart Circ Physiol* 287: H1115–H1124, 2004. First published May 13, 2004; 10.1152/ajpheart.00075.2004.—Mechanisms mediating vascular calcification remain incompletely understood. Nanometer scale objects hypothesized to be a type of bacteria (nanobacteria) are associated with calcified geological specimens, human kidney stones, and psammona bodies in ovarian cancer. Experiments were designed to evaluate human vascular tissue for the presence of similar nanometer-scale objects. Calcified human aneurysms ($n = 8$), carotid plaques ($n = 2$), femoral arterial plaques ($n = 2$), and cardiac valves ($n = 2$) and noncalcified aneurysms from patients with bicuspid aortic valve disease ($n = 2$) were collected as surgical waste from the Heart Hospital of Austin, Austin, Texas, and Mayo Clinic, Rochester, Minnesota. Whole mounts or adjacent sections from each specimen were examined by electron microscopy, stained for calcium phosphate, or stained with a commercially available antibody (8D10). Filtered (0.2 μm) homogenates of aneurysms were cultured and costained with 8D10 antibody followed by PicoGreen to detect DNA or incubated with [^{3}H]uridine. Staining for calcium phosphate was heterogeneously distributed within all calcified tissues. Immunological staining with 8D10 was also heterogeneously distributed in areas with and without calcium phosphate. Analysis of areas with positive immunostaining identified spheres ranging in size from 30 to 100 nm with a spectral pattern of calcium and phosphorus (high-energy dispersive spectroscopy). Nanosized particles cultured from calcified but not from noncalcified aneurysms were recognized by a DNA-specific dye and incorporated radiolabeled uridine, and, after decalcification, they appeared via electron microscopy to contain cell walls. Therefore, nanometer-scale particles similar to those described as nanobacteria isolated from geological specimens and human kidney stones can be visualized in and cultured from calcified human cardiovascular tissue.

aneurysm; chlamydia; infection; inflammation; nanobacteria

ATHEROSCLEROSIS is an inflammatory disease caused in part by abnormal lipid metabolism within the arterial wall (44). However, evidence also suggests that microbial infection contributes to inflammation and disease progression (8, 42, 51) as the risk for adverse cardiovascular events increases with infectious burden (7, 15–17, 22, 31), and individuals with polymorphism Asp299Gly of the Toll-like receptor 4 (the receptor for pathogen-derived lipopolysaccharide), although susceptible to infection, are at decreased risk for atherosclerosis (2, 32). However, little is known about whether or not and/or how pathogenic infections affect calcification processes within arteries.

Calcification of human arterial tissue within atherosclerotic plaques is a common occurrence, increases with age, and is a strong predictor of cardiovascular and all-cause mortality (4, 23). Several hypotheses regarding the pathogenesis of vascular calcification have been proposed, including *1*) that crystals deposit on degrading senescent cells (matrix vesicles) (25, 33, 34), *2*) that nucleate amorphous hydroxylapatite on phospholipids and proteoglycans (34), *3*) that cellular alkaline phosphatases and/or phosphate-specific channels are stimulated resulting in critical escalation of local saturation levels (39, 46), or *4*) and that smooth muscle cells undergo bonelike differentiation (46, 47).

Nanoparticles associated with precipitation of calcium carbonate were first discovered by geologists in natural hotspring deposits at Viterbo, Lazio, Italy and named for their small size (0.03–0.3 μm) (18, 19). Similar structures have been isolated from human blood, urine, renal cyst fluid, and kidney stones (24, 28, 29) and demonstrated by electron microscopy in psammoma bodies of ovarian cancer (45), suggesting that these structures may contribute to calcifying diseases in humans. These nanoparticles appear to be self-replicating in culture (28, 29), and therefore it has been hypothesized they are nanometer-scale bacteria or "nan(n)obacteria." Nanoparticles from geological specimens petrify with calcium carbonate, silica, iron sulfide, and complex silicates as well as phosphate (18, 19), whereas nanoparticles isolated from mammalian kidney stones are encapsulated with hydroxylapatite, the calcium mineral found in atherosclerotic tissue (28).

Growth of nanobacteria/particles in culture depends on the culture media (28, 29, 50). Cultures are relatively resistant to a variety of agents, including ultraviolet irradiation and heat, but are sensitive to antimicrobial agents (3, 10). However, controversy remains as to whether or not cultured nanoparticles are unique living organisms, in part, because of their very small size, and because a unique genetic material (DNA or RNA) has yet to be isolated (11). Nevertheless, it is attractive to hypothesize that arterial calcification might be caused, in part, by nano(bacteria) particles. To test this hypothesis, experiments

Address for reprint requests and other correspondence: V. M. Miller, Medical Science Bldg. 4-62; Mayo Clinic Rochester; 200 First St. SW, Rochester, MN 55905 (E-mail: miller.virginia@mayo.edu).

The costs of publication of this article were defrayed in part by the payment of page charges. The article must therefore be hereby marked "*advertisement*" in accordance with 18 U.S.C. Section 1734 solely to indicate this fact.

were designed to examine anatomic, immunological, and biological evidence for nanoparticles in calcified arterial and valvular human tissue.

MATERIALS AND METHODS

Tissue

Calcified human carotid plaques ($n = 2$), abdominal aortic aneurysms ($n = 8$), cardiac valves ($n = 2$), and femoral arterial plaques ($n = 2$) were collected as surgical waste from patients undergoing vascular/valvular repair at the Heart Hospital of Austin, Austin, TX, and Mayo Clinic Rochester, Rochester, MN. Ages of patients ranged from 52 to 92 yr, and risk factors for cardiovascular disease included hypertension, diabetes, smoking, and hyperlipidemia (Table 1). A segment of aorta from a patient who died of trauma and who had no evidence of cardiovascular disease was used as control tissue for histology. For culture experiments, noncalcified pieces of ascending aorta were obtained from patients ($n = 2$) undergoing repair of ascending aortic aneurysm and annuloaortic ectasia resulting from bicuspid aortic valve disease (a congenital anatomic defect). For histologic assessment, tissues were collected into glutaraldehyde or Trump's fixative (1% glutaraldehyde and 4% formaldehyde in 0.1 M phosphate buffer, pH 7.2). For culture, specimens were collected into sterile saline.

Scanning Electron Microscopy

For whole mounts, tissues were dehydrated through ethanol and acetone and critically point dried. Specimens were sputter coated with gold-palladium for <30 s because metallic coating for longer than 30 s produces artifacts (21). For energy dispersive X-ray microanalysis, tissues were coated with carbon. Micrographs were obtained on a JSM-T330A (University of Texas) operating at 30 kV at up to ×200,000, and on a Hitachi S4700 FESEM operating at 5 or 20 kV (Electron Microscopy Core, Mayo Clinic). Scanning electron microscopy also was performed on paraffin-embedded tissue sections (see *Light Microscopic Analysis of Tissues*).

Light Microscopic Analysis of Tissues

To prepare sections, tissue segments adjacent to the whole mount segments were embedded in paraffin, sectioned (5 μm), and mounted on glass slides for staining with silver nitrate for calcium phosphate (von Kossa), for apoptosis using terminal deoxynucleotidyl transferase (TdT)-mediated dUTP-biotin nick-end labeling (TUNEL, ApopTag, Serologicals; Norcross, GA), or for nanoparticles using a monoclonal antibody raised against bovine nanobacteria (8D10; 10 μg/ml; Nanobac Oy; Kuopio, Finland).

For TUNEL staining, rat mammary tissue was used for positive controls, and sections not exposed to TdT enzyme served as negative controls. Images were viewed using a Zeiss, Axiovert 135 TV microscope, and images were captured and stored using Axiocam with Axiovision 3.1 program.

The 8D10 antibody was obtained from hybridoma clones of mouse splenocytes immunized with cultured nanoparticles of bovine origin and fused with myloma strain P3x63-Ag8.653. The antibody is thought to be directed toward a porin protein epitope (24). Immunostaining was performed on paraffin-embedded sections (5 μm). Staining procedures using the 8D10 antibody were as recommended by the manufacturer omitting the EDTA treatment step. Staining sensitivity was increased using the catalyzed signal amplification kit (CSA; DAKO, Carpinteria, CA). Sections were immunoabsorbed with IgG (matching isotype) as negative controls for the antibody. In preliminary experiments, adjacent sections were stained with an antibody against human α-thrombin (EST-4, American Diagnostica) and *Chlamydia pneumoniae* (Clone RR-402, Washington Research; Seattle, WA) to detect possible colocalization. To exclude the possibility that the antibody chemically interacted with calcium, additional adjacent sections of all tissues were decalcified before being stained with the 8D10 monoclonal antibody by using 20% formic acid for 12–18 h followed by a running tap water rinse for 30 min. Decalcified tissues did not contain calcium phosphate (von Kossa stain).

Table 1. *Patient demographics*

Risk Factors	Women ($n = 6$): 57–92 yr old	Men ($n = 8$): 52–80 yr old
Hypertension	5	4
Diabetes	0	2
Smoking	4	6
Hyperlipidemia	4	5

Values represent the number of patients.

Culture of Nanoparticles

Filtered homogenates were prepared from calcified abdominal aortic aneurysms and noncalcified thoracic aneurysms from patients with bicuspid aortic valve disease removed at the time of vascular surgery. Tissues were homogenized using an 18-gauge needle. This homogenate was forced through a 0.2-μm filter to remove arterial cells and bacteria >200 nanometers in size. The filtrate was then inoculated into 10-ml vented tissue culture flasks (Corning; Corning, NY) and 10 ml of Dulbecco's modified Eagle's medium (DMEM) containing 10% γ-irradiated calf serum (Sigma; St. Louis, MO). After several weeks, optical density of the inoculated media increased more than twofold. Motile particles <1 μm in size were observed by phase-contrast microscopy. Every 4–6 wk, flasks were scraped with a rubber spatula and divided 1:10 into fresh DMEM containing 10% γ-irradiated calf serum for subculture. The optical density did not increase nor were motile particles observed in uninoculated flasks containing media alone. Cultures were negative when screened for *Mycoplasma* by using a sensitive rapid PCR test performed in the Mayo Clinic Microbiology Laboratory.

To detect uridine incorporation into nucleic acids, cultures were diluted 1:10 into DMEM containing 10% γ-irradiated calf serum. This dilution was spiked with [^{3}H]uridine (50 μCi in 6 ml; American Radiolabeled Chemicals; St. Louis, MO), and 200-μl aliquots were placed in quadruplicate into the inner 24 wells of a 96-well plate (Falcon, Becton-Dickinson; Franklin Lakes, NJ). Surrounding wells were filled with sterile water to limit evaporation during the experiment, and the plate was maintained at 37°C in a 13% CO_2 incubator. Entire plates were processed for [^{3}H]uridine incorporation daily beginning *day 0* through *day 3*. To precipitate nucleic acids and dissolve calcium phosphate, 20% trichloroacetic acid (TCA; 200 μl) was added to wells containing samples, which were incubated overnight at 4°C. To count radioactivity, the precipitates and wash of each well (400 μl of 10% TCA) were captured on GF/A Whatman filters (Whatman International; Maidstone, UK), which were washed with 100% ethanol and counted by using Ultra Gold (6 ml, Packard; Meriden, CT). Cultures containing DMEM, 10% γ-irradiated calf serum, and an equivalent amount of autoclaved inorganic hydroxyapatite crystals (121°C for 1 h, Sigma) were used as a negative control.

Electron Microscopy of Cultured Nanoparticles

Four flasks of nanoparticles demonstrating good growth were scraped and centrifuged at 150,000 *g* for 40 min. For scanning electron microscopy of calcified samples, the resulting pellet was rinsed with double distilled H_2O and air dried on a glass coverslip. To visualize underlying structures, the resulting pellet was decalcified in EDTA (0.5 M, pH 8 at 4°C overnight) and passed through a 0.1-μm filter (Millipore; Bedford, MA). The filter was critically point dried

and sputter coated with gold-palladium for <30 s. For transmission electron microscopy (TEM), the resulting pellet was fixed in Trump's fixative and embedded in agarose. Samples were postfixed with osmium, dehydrated, embedded in Spurr, sectioned, stained with uranyl acetate and lead citrate, and examined using a JEOL Ex11 TEM.

For immunogold staining, antigen retrieval was performed by incubating grids with SDS for 30 min at room temperature. All grids were incubated in 1% glycine for 15 min to block free aldehydes that can be introduced by aldehyde fixation. After a brief water rinse, grids were incubated in PBS plus 0.05% Tween 20 (PBST) with normal goat serum for 15 min. Grids then were incubated in the absence (negative control) or presence of the primary antibody 8D10 diluted 1:2 in PBST for 3 h at room temperature. Grids were rinsed thoroughly in PBST and incubated 60 min in goat anti-mouse conjugated to 5 nm colloidal gold. Sections were rinsed thoroughly in PBST and water, silver enhanced, stained with uranyl acetate and lead citrate, and examined by TEM.

Immunostaining and DNA staining of cultured nanoparticles. To characterize the specificity of the 8D10 antibody, a protein extract was prepared from ten 10-ml flasks of cultured nanoparticles. Flasks were scraped, and the medium was transferred to centrifuge tubes to prepare a pellet (9,000 *g* for 60 min), which was then decalcified in 0.3 M EDTA, pH 8.0, overnight. Decalcified nanoparticles were then pelleted (64,000 *g* for 60 min), solubilized in Laemelli buffer, resolved by SDS-PAGE, and electroblotted to a polyvinylidine fluoride membrane. The blot was probed with the 8D10 antibody. As a negative control, a protein extract was prepared from DMEM plus 10% γ-irradiated calf serum seeded with inorganic hydroxyapatite crystals.

For immunostaining of cultures, a pellet was prepared by centrifuging turbid, inoculated flasks (100,000 *g* for 20 min). Pellets were diluted in 10 mM Tris, 150 mM NaCl, and 1 mM EDTA (pH 7.5) (TNE) buffer (100 μl, Molecular Probes; Eugene, OR), spread on a glass coverslip, air dried, and incubated for 5 min at 60°C. Nanoparticles were fixed and permeabilized by incubation for 10 min in a 3.7% formaldehyde solution containing 0.2% Triton X-100. The coverslips were then gently washed twice with PBS (pH 7.4) for 5 min each. To block nonspecific binding sites, coverslips were incubated for 1 h with 1% goat serum, which was aspirated and replaced with 8D10 antibody (100 μg/ml for 1 h). Coverslips were then washed four times with PBS (5 min each) and incubated for 45 min with anti-mouse antibody conjugated with Texas red (10 μg/ml). The antibody was aspirated, and coverslips were washed four times with PBS (5 min each). For DNA staining, coverslips were incubated in the dark for 30 min with PicoGreen dye (Molecular Probes) that was diluted 1/100 in TNE buffer. Coverslips were then washed four times with PBS (5 min each). All samples were mounted onto slides using Slow-Fade (Molecular Probes) and viewed on a Nikon ECLIPSE E600 fluorescent microscope equipped with a Nikon DXM1200 digital still camera (Nikon Instruments, Melville, NY).

RESULTS

Electron and Light Microscopic Analysis of Whole Mounts and Tissue Sections

All diseased atherosclerotic tissues contained macroscopic evidence of calcification (Fig. 1), as opposed to those removed for bicuspid aortic valve disease, which therefore served as a control for culture (see below). Upon scanning electron microscopy analysis of whole mounts of abdominal aortic aneurysms, diseased areas were characterized by at least two distinct anatomic patterns. One area lacked distinct structures and was defined by amorphous material that did not show a calcium peak by X-ray microanalysis (Fig. 1, *middle*). Beneath a ridge at the calcium-tissue interface a second pattern characterized by distinct 0.5- to 1.2-μm spheroidal structures was observed. These structures had a mottled appearance and were of a size comparable to that described for nanobacteria (19). With the use of X-ray microanalysis, structures displayed discrete peaks for calcium and phosphorus (Fig. 1, *bottom*).

Scanning electron microscopy of other tissues revealed discrete variations in the density of the spherical structures (Fig. 2). Valvular tissue contained spheroids ranging in size from 30 to 100 nm in diameter that were distributed throughout calcified and noncalcified areas of the same valve and were of variable density. Even in areas that did not demonstrate macroscopic signs of calcification, regions containing smooth finger-like projections (100 nm wide and up to 500 nm long) and spheroids (100 nm) were observed (Fig. 2, *left*). In other regions of the same valve, these spheres appeared as isolated balls, irregular clumps, rosary-like chains, monolayer sheets or solid masses, and sheets of hydroxylapatite balls. Sheetlike structures observed in valvular tissue were similar to those observed in aneurysmal tissues (Fig. 2, *middle* and *right*).

In general, all tissues that demonstrated macroscopic evidence of calcification contained areas that stained positively both with von Kossa stain and the 8D10 antibody. However, 8D10 staining was heterogeneously distributed throughout the tissues, and areas recognized by the 8D10 antibody did not always coincide with calcium phosphate (von Kossa stain). A representative pattern of staining is shown in Fig. 3. In this diseased femoral artery, calcium phosphate was visualized within an atheroma and at the media-plaque border (Fig. 3, *left*). Certain regions recognized by the 8D10 antibody coincided with positive staining for calcium phosphate (Fig. 3, *right*). However, the 8D10 antibody also recognized areas without calcium phosphate, often in the vicinity of cholesterol clefts (Fig. 3, *right*).

In general, the 8D10 antibody recognized regions within fibrous caps, at the borders of certain cholesterol clefts, and at the interface between the media and atheromas (Fig. 4, *left*).

Matrix vesicles, perhaps derived from apoptotic cells, have been implicated in arterial calcification (25, 33, 34). In sections of aneurysm and femoral arteries, occasional cells within the fibrous cap, media, and/or adventitia demonstrated TUNEL staining, with the majority of positive cells localized to the adventitia. Importantly, TUNEL and 8D10 staining never colocalized (Fig. 4, *middle*). Therefore, the distribution of TUNEL staining (apoptotic bodies) and 8D10 staining (nanoparticles) clearly differed. In addition, antibodies against human α-thrombin and *C. pneumonia* recognized structures in the media, and the pattern did not coincide with that recognized by the 8D10 antibody (not shown). Importantly, immunostaining using 8D10 was still observed after calcified, diseased tissues were decalcified and was absent in an aorta derived from a young trauma victim (not shown).

At an accelerated voltage of 20 kV, areas recognized by the 8D10 antibody displayed a bright signal consistent with calcium (Fig. 4, *right*). Higher magnification of these areas revealed discrete, sphere-like structures ranging in size from 200 to 300 nm with mottled surfaces (Fig. 4, *right*, *inset*). Similar patterns were observed in plaques from the aneurysm and femoral and carotid arteries (not shown).

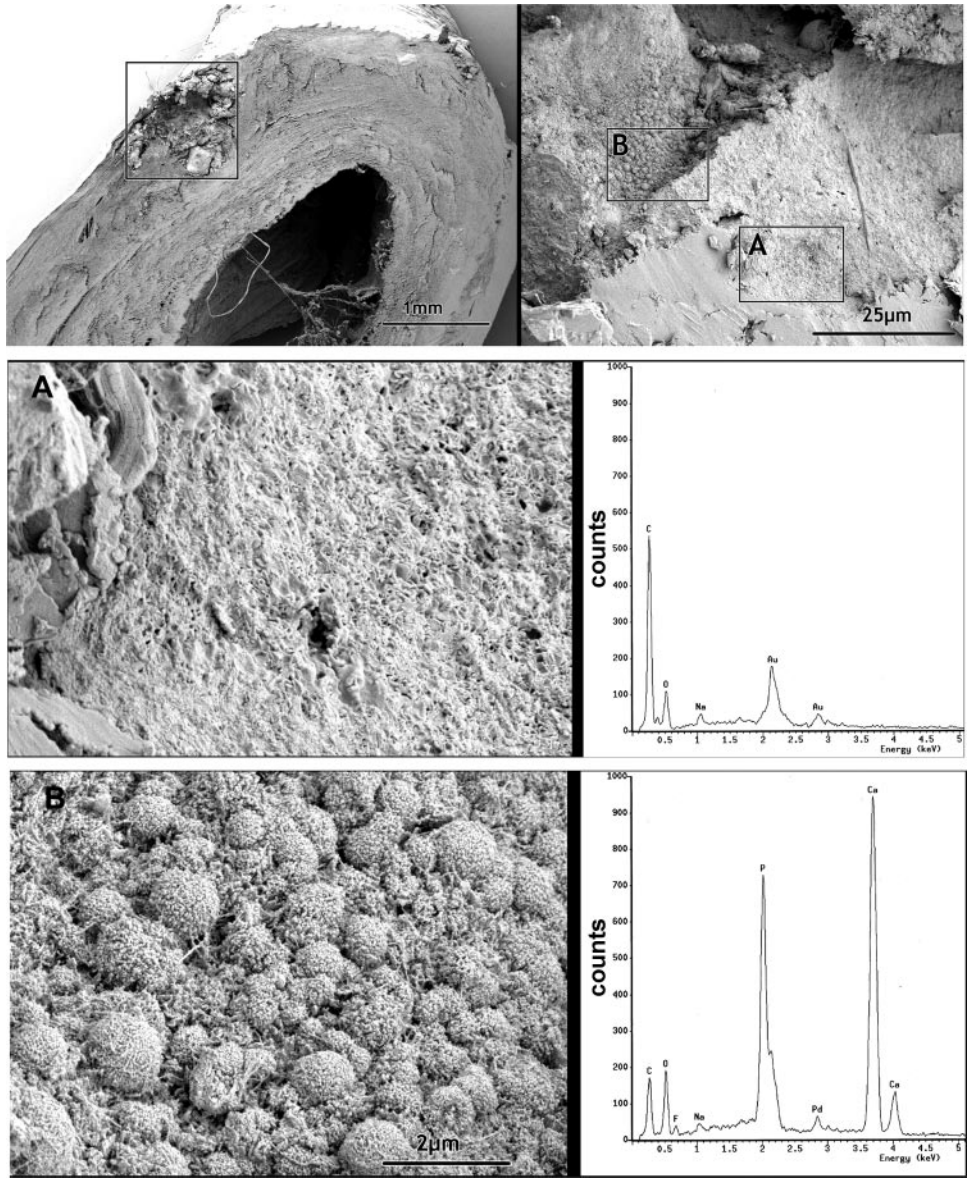

Fig. 1. *Top*: representative scanning electron micrographs (SEM) of a whole mount of an abdominal aortic aneurysm. Bar indicates magnification. Box area (*left*) represents area of calcification. This area, when enlarged (*right*), shows spherelike structures at the tissue-calcification interface. Higher magnification of *A* and *B* are shown in the *middle* and *bottom*, respectively. X-ray microanalysis (*right*) of *A* did not reveal discrete calcium peaks, whereas *B* showed discrete nanosphere structures and X-ray microanalysis of the spherical structures revealed both calcium and phosphorus peaks.

Analysis of Cultures Derived From Filtered Tissue Homogenates

Anatomy. Not all filtered (0.2 μm) tissue homogenates resulted in robust growth of nanoparticles. Filter tissue homogenates of nondiseased ascending aorta from patients with bicuspid aortic valve disease ($n = 2$), which were noncalcified, did not demonstrate growth. However, particles were cultured from filtered homogenates of calcified abdominal aortic aneurysms ($n = 2$), and these cultures shared anatomic characteristics with nanoparticles cultured from bovine serum (Fig. 5). After decalcification with EDTA and critical point drying, underlying membranous structures could be observed by scanning electron microscopy (Fig. 6). No structures were observed in flasks containing media alone. By TEM, cultured particles contained a crystalline shell that appeared to surround an inner structure (Fig. 7, *left*). In addition, immunogold-labeled 8D10 antibody recognized these structures within a culture biofilm in vitro (Fig. 7, *right*).

Specificity of 8D10 antibody. Several proteins were observed when protein extract from cultured, decalcified nanoparticles was resolved by SDS-PAGE gel (Fig. 8, *lane 2*). However, the monoclonal antibody 8D10 recognized a single ~50-kDa band in a Western blot analysis (Fig. 8, *lane 3*). Importantly, this ~50-kDa band was not detected by the 8D10 antibody in extracts derived from decalcified synthetic hydroxyapatite crystals incubated in DMEM and γ-irradiated calf serum (not shown). The pattern of proteins eluted from inorganic hydroxyapatite crystals was also entirely different, with a large predominant protein band at ~80 kDa. Therefore, although it cannot be certain that the band recognized in Fig. 8 is a single protein, available evidence does suggest that the 8D10 antibody recognizes a ~50-kDa protein present in nanoparticles that is not derived from calf serum.

Evidence that cultured particles contain nucleic acids. Structures cultured from the filtered tissue homogenates, also recognized by the 8D10 antibody, were stained with a dye for

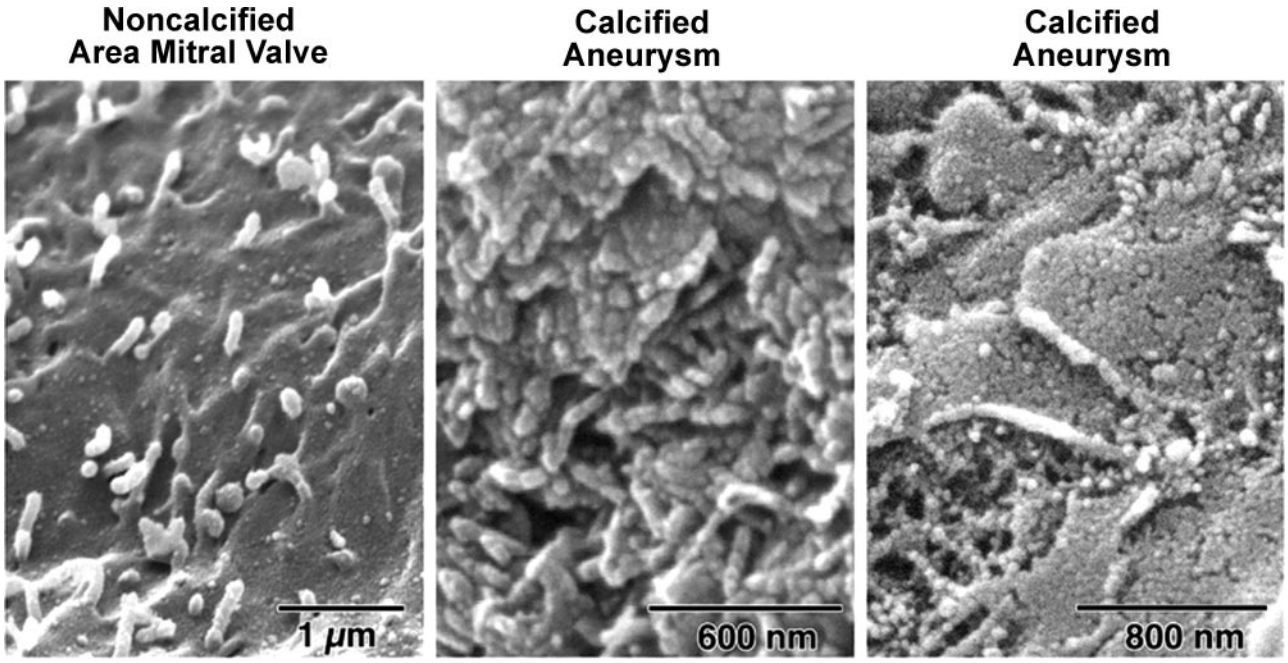

Fig. 2. Representative SEM of a mitral valve (*left*), and calcified aneurysm (*middle* and *right*). The finger-like projections seen on this mitral valve, 100 nm wide and up to 500 nm long, were from a region without overt calcification, and ultrastructurally appear similar to the "nanobes" isolated from sandstone (see Ref. 49). In this aneurysm sample, spheres of 25–60 nm were randomly arranged either side by side (*middle*) or in sheets (*right*). Similar structures were observed on another calcified valve (not shown). Bar indicates micrometer scale.

DNA (PicoGreen) in a pattern that colocalized (Fig. 9). These cultures also incorporated radiolabeled uridine in a time-dependent manner over 3 days (Fig. 10), providing evidence of ongoing nucleic acid synthesis.

DISCUSSION

This study provides anatomic evidence that calcified human arterial and valvular tissue contain nanometer-sized particles that share characteristics of nanoparticles recovered from geological specimens, mammalian blood, and human kidney stones (1, 18–21, 28, 35, 49) and were observed by transmission electron microscopy in a calcified human mitral valve (27). The anatomic and ultrastructural evidence of the existence of nanoparticles in calcified human tissue is supported and strengthened in the present study by immunohistochemical microscopy and in vitro culture of nanoparticles.

Immunohistochemical evidence for nanoparticles was obtained using the commercially available antibody 8D10 raised

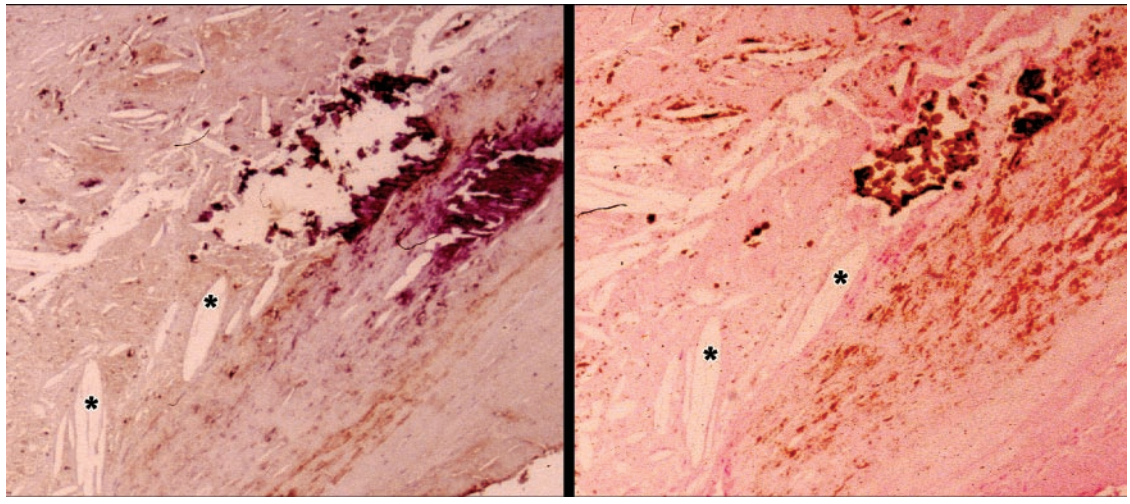

Fig. 3. Representative light micrographs of a section (5 μm) through a calcified human femoral artery. Discrete areas of calcification are identified by von Kossa staining (*left*). Positive staining (brown) using a monoclonal antibody raised against bovine nanobacteria (8D10; 1:10 dilution) demonstrated positive staining both within and adjacent to areas associated with calcium phosphate (von Kossa stain) (*right*). *Cholesterol clefts appear clear. Sections immunoabsorbed for IgG demonstrated no staining for 8D10 antibody (not shown). Similar results were observed in sections of another femoral artery, cardiac valve, carotid artery, and eight aneurysms.

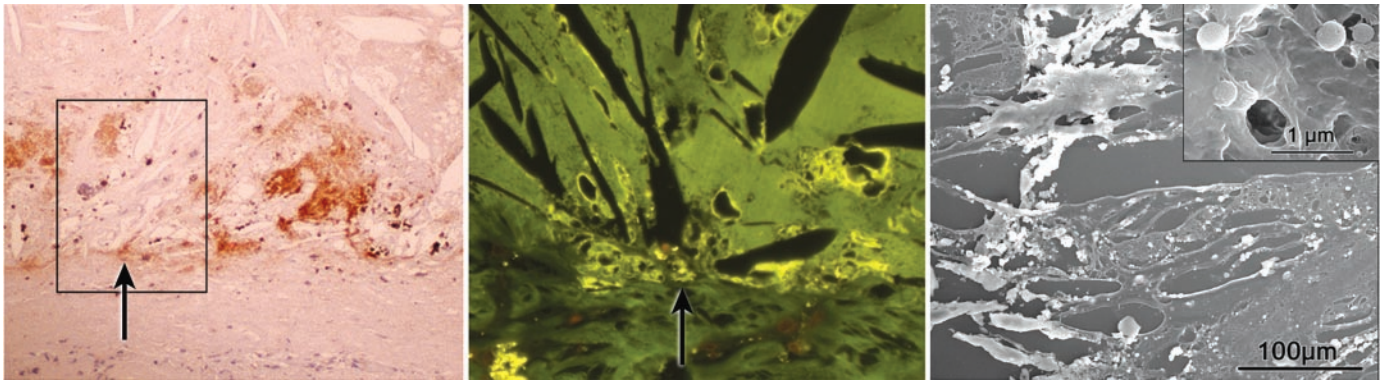

Fig. 4. Representative light and SEM micrographs of a section (5 μm) of a calcified human aortic aneurysm. One section (*left*, ×200) was stained with the monoclonal antibody raised against bovine nanobacteria (8D10; 1:10 dilution). Positive staining appears brown (*left*). Sections immunoabsorbed with IgG demonstrate no staining (not shown). An adjacent section was stained for apoptosis with terminal deoxynucleotidyl tranferase-mediate dUTP-biotin nick-end labeling (TUNEL) [*middle*; image was viewed using a Zeiss, Axiovert 135 TV microscope (×200) captured and stored using Axiocam with Axiovision 3.1 program]. No positive staining with TUNEL was observed in a region that showed positive staining for 8D10. *Left inset*, landmark for scanning by electron microscopy (*right*). A separate adjacent section was lightly sputter coated with gold-palladium. With the use of an accelerated voltage (20 kV), calcium deposits generated a stronger signal compared with the other areas of the sample. Bright areas revealed a pattern consistent with calcium phosphate. Upon higher magnification (*right inset*), spheres in the range of 200–300 nm with mottled surfaces were observed. Note the smaller cluster of 50-nm structures beneath the sphere in the upper right corner and at the end of the bar marker. Similar results were observed in sections of another aneurysm and in femoral arterial plaques and carotid arteries.

against bovine nanobacteria. Positive staining with the 8D10 antibody was observed in all tissues in which calcium phosphate was confirmed by von Kossa staining. Because positive staining with the 8D10 antibody was also observed in noncalcified areas of diseased tissue, it is plausible that nanoparticles may be present during early stages of the calcification process. Although the protein identified by this antibody remains to be identified, it is unlikely that staining is due to a chemical interaction of the antibody with calcium, because 8D10 antibody staining was still detected when diseased tissues were decalcified. It is also unlikely that the antibody detected only apoptotic cells because the distribution of TUNEL-positive cells did not overlap with 8D10-positive structures.

It is equally unlikely that the antibody recognizes only matrix vesicles, extracellular microstructures derived from chondrocyte plasma membrane and associated with osseous calcification, because matrix vesicles do not contain DNA or replicate in culture (5, 6, 52). The 8D10 antibody stained nanoparticles in culture, which costained with PicoGreen, indicating the presence of DNA. In addition, TEM of cultures stained with immunogold-labeled 8D10 antibody showed specific, albeit sparse, labeling associated with nanoparticles and biofilm. Because immunogold processes may affect binding sites for either antibody or antigen, intensity of staining may not be representative of binding in the absence of the gold label.

The biological nature of nanometer-sized particles remains controversial (14, 30, 38, 40). Drancourt and colleagues (14), while identifying nanosized particles in human kidney stones, were unable to propagate these structures in culture (14). Alternatively, Cisar and colleagues (11) were able to propagate nanosized particles from human saliva using conditions described by Kajander and Ciftcioglu (28) but were unable to detect novel DNA. Therefore, they concluded that nanobacteria represent a form of biomineralization initiated by nonliving macromolecules, perhaps similar to matrix vesicles (33). In the present experiments, recognition by the 8D10 antibody of protein derived from extracts of cultured nanoparticles was distinct from those derived from culture media conditioned with hydroxyapatite, suggesting that structures cultured from

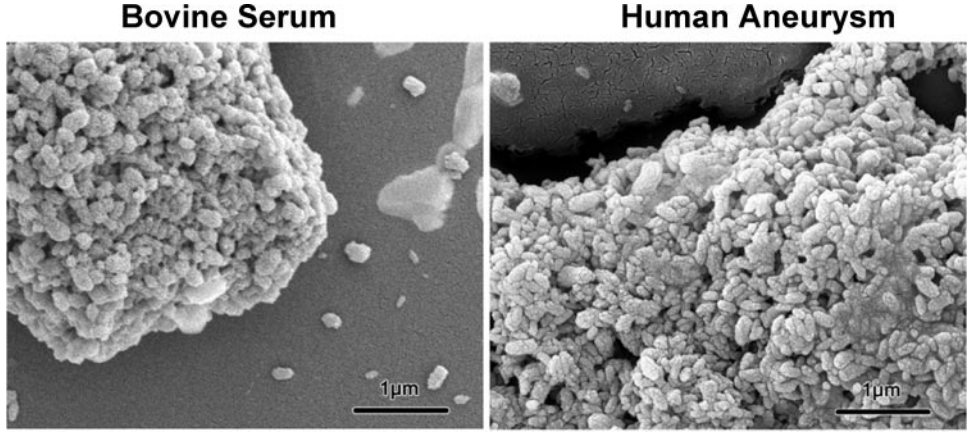

Fig. 5. SEM of cultures of nanoparticles derived from bovine serum and from filtered homogenates of aortic aneurysm. The culture from bovine serum was a positive control provided by the manufacturer of antibody 8D10 (Nanobac Oy). Similar cultures were obtained from another filtered homogenate of an aneurysm. Bar indicates micrometer scale.

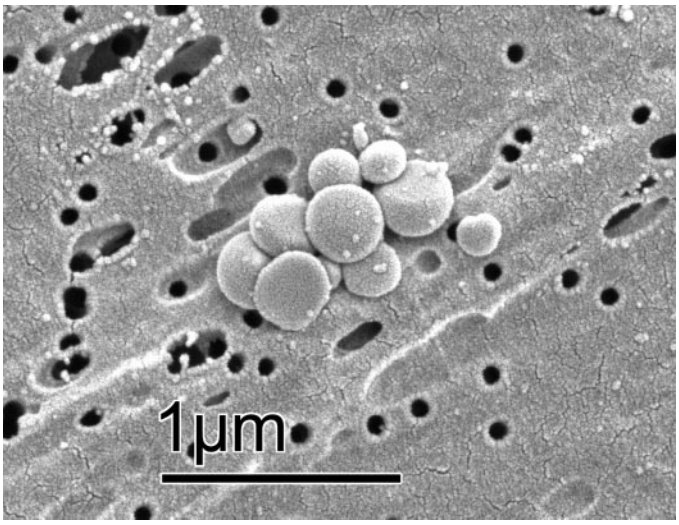

Fig. 6. SEM of decalcified cultured nanoparticles reveals spherical structures 100–200 nm in size. Background is the filter. Bar is micrometer scale.

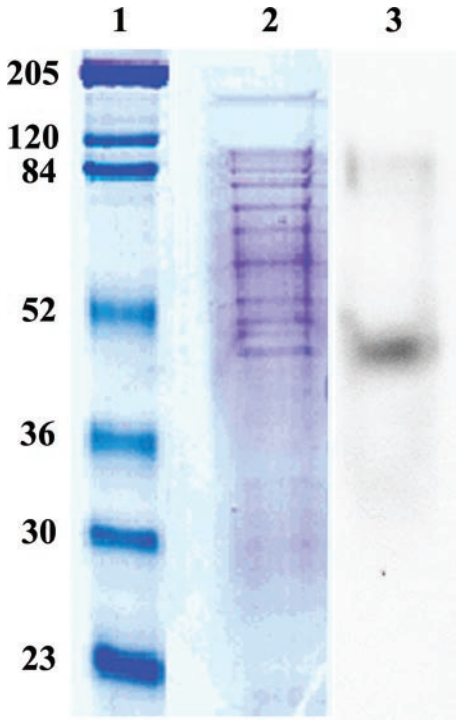

Fig. 8. Composite figure of a SDS-PAGE gel (*lane 2*) and Western blot analysis (*lane 3*) of proteins derived from nanoparticles cultured from filtered homogenates of human aneurysm. A single band of protein (relative molecular mass ~50 kDa) is identified by the monoclonal antibody 8D10 (*lane 3*) in a protein extract of cultured nanoparticles (*lane 2*) that corresponds to ~50 kDA of the standard proteins (*lane 1*). The 8D10 antibody did not recognize any protein band in extracts derived from media conditioned with inorganic hydroxyapatite crystals (not shown).

filtered homogenates of calcified human abdominal aortic aneurysms were not the result of mineralization alone. Furthermore, nanoparticles cultured from homogenates of calcified aneurysms stained with a probe for DNA, suggesting they contain nucleic acids. These observations are consistent with those of other investigators who have cultured nanometer-sized structures containing nucleic acids from Australian sandstone (49), human kidney stones (28), and mammalian blood (1, 28, 50). It is unlikely that the nanoparticles cultured from filtered tissue homogenates were the result of contamination for several reasons. Viable cultures were obtained from calcified but not from noncalcified aneurysms. In addition, uninoculated cultures containing DMEM and γ-irradiated calf serum did not demonstrate growth as indicated by increases in optical density, even when the medium was seeded with inorganic hydroxyapatite crystals. Furthermore, the 8D10 antibody did not recognize protein from control cultures containing media and inorganic hydroxyapatite. These control cultures did not show incorporation of radiolabeled uridine comparable to cultures inoculated with nanoparticles.

Although a unique nucleic acid sequence remains to be identified from the nanosized particles identified within human arterial tissue in the present report, it is possible that these structures may represent either a variant form of microorganisms or an unrecognized bacterial growth stage (12, 29) such as L-forms, cell wall-deficient bacteria, and/or defective bacteria that have been hypothesized to represent either pleuropneumonic-like organisms or *Mycoplasma* species, which have been detected in serum of patients with long histories of chronic diseases (13). They may also represent an Archaea symbiont that requires cell contact or lipids from other cells for growth. The latter possibility is supported by the very small size, which suggests these organisms may lack certain gene products. Of note in the present study, immunological staining was observed in association with cholesterol clefts and at the interface between medial tissue and atheromic material. Nanosized hyperthermophilic Archaea contain unique ribosomal RNA and may share a symbiotic existence with other micro-

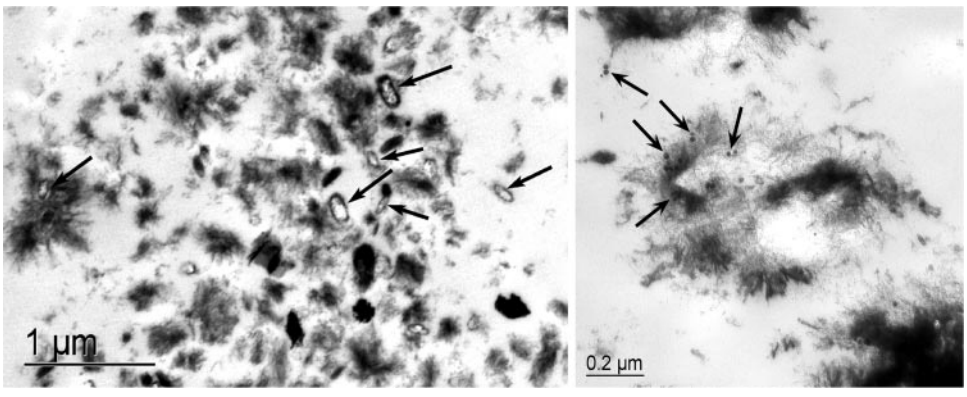

Fig. 7. *Left*: transmission electron microscopy (TEM) of calcified nanoparticles (shown in Fig. 5) with arrows denoting structures resembling cell walls. *Right*: TEM sections were stained with immunogold-labeled 8D10 antibody. Arrows denote structures with boundaries resembling cell walls (*left*) and of immunogold label (*right*). Bar indicates micrometer scale.

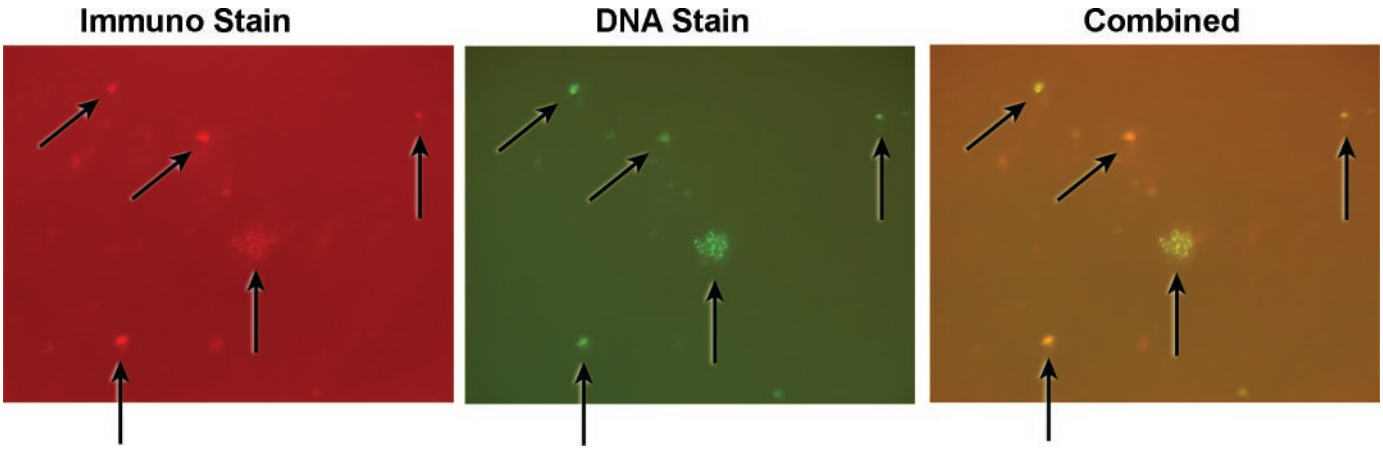

Fig. 9. Immunostaining of structures cultured from filtered, homogenates of human aneurysm shown in Fig. 6. *Left*: positive staining (bright red fields, arrows) using the monoclonal antibody 8D10; *middle*: positive staining using the DNA probe PicoGreen (green, arrows); *right*: overlay of both antibody 8D10 and PicoGreen. PicoGreen staining is superimposed on staining for 8D10 (yellow, arrows).

organisms (26). Perhaps relevant, cholesterol is associated with progression of valvular calcification (41). Nucleic acid sequences have been identified from marine bacterioplankton, which have an estimated cell volume of about 0.01 μm^3, similar to the size of nanoparticles (43).

Vascular calcification is a multifactorial process. It should be emphasized that the results of the present study do not negate the possible contribution to mineralization processes of matrix vesicles, the chemical interactions of calcium with membrane-derived matrix vesicles (33, 34, 39), nor of differentiated osteogenic cells within the vessel wall (48). Results, however, suggest that an additional biological factor might contribute to the calcification of arterial tissue. Nanobacteria derived from bovine serum are internalized by human cells and appear to be cytotoxic (9). Similar internalization of nanolike particles in arterial smooth muscle would be consistent with induction of apoptosis (36), formation of matrix vesicles (37), and the inflammatory basis of atherogenesis (44). An infectious etiology of arterial calcification is consistent with increased lesion formation in experimental models of atherosclerosis (8).

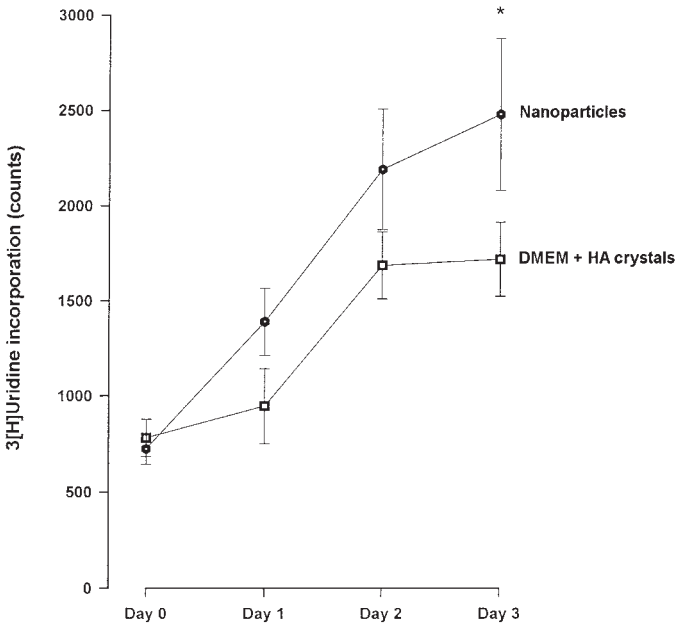

Fig. 10. Incorporation of [^{3}H]uridine by cultures of nanoparticles derived from filtered homogenates of human aneurysm (nanoparticles). Control cultures contained DMEM and γ-irradiated calf serum plus inorganic hydroxyapatite (HA) crystals. Data are shown as amount of radioactivity of two separate experiments conducted in quadruplicate (means ± SE). Uptake of radiolabeled uridine by nanoparticles was 56% greater than control cultures after 3 days. *$P < 0.05$ vs. control.

In the current experiments, a potential pathogen was associated with arterial and valvular calcification. These calcified DNA-containing nanoparticles were also cultured from filtered homogenates of calcified vessels but not of noncalcified control aorta. However, a definitive cause and effect relationship needs to be established between these nanoparticles and vascular calcification. For example, it will be necessary to evaluate severity of calcification and disease progression in the absence, presence and titer of nanoparticles in humans. In the experimental setting, it will require infection of a naïve animal with cultured nanoparticles and subsequent identification of the particles within arterial calcification. Definitive characterization of these unique particles will require isolation and sequencing of genetic material (DNA or RNA).

In summary, sphere-like structures ranging in size from 30 to 150 nm and finger-like rod structures were identified in calcified human tissue of four different origins: carotid plaque, cardiac valve, aortic aneurysm, and femoral arterial plaque. These structures exist in areas containing calcium phosphate by von Kossa staining and X-ray microanalysis and resemble "nan(n)obacterial" structures observed in calcified geological specimens (19), structures described as "nanobacteria" that were cultured from kidney stones (28) and "nanobes" cultured from Australian sandstone (49). Self-replicating structures containing nucleic acids were also cultured from filtered homogenates of two calcified aneurysms. However, direct cause and effect relationship between these culturable particles and calcifying disease remains to be determined.

ACKNOWLEDGMENTS

The authors gratefully acknowledge K. Milliken of the Department of Geosciences, J. Mendenhall of the Microscopy Laboratory of the Institute for Cellular and Molecular Biology at the University of Texas at Austin, and J. Uhl

of the Mayo Clinic Department of Laboratory Medicine and Pathology for advice and assistance. We also thank Drs. Olavi Kajander and Neva Ciftcioglu for helpful discussions.

Present address of B. Kirkland: Department of Geosciences, Room 208, Hilbun Hall, University of Mississippi, Mississippi State, MS 39762.

Present address of T. E. Rasmussen: Uniformed Services University of the Health Sciences, 4301 Jones Bridge Road, Bethesda, MD 20814.

E. Rzewuska-Lech was a Fulbright Visiting Scholar from Poland. Her present address is Etiudy Rewolucyjnej 15/17/1, 02-643 Warsaw, Poland.

GRANTS

This work was funded in part by grants from the National Institutes of Health (DK-62021), Mayo Foundation, Ralph C. Wilson Sr. and Ralph C. Wilson Jr. Medical Research Foundation, and Austin Heart Foundation.

REFERENCES

1. **Akerman KK, Juronen I, and Kajander EO.** Scanning electron microscopy of nanobacteria: novel biofilm producing organisms in blood. *Scanning Electron Microscopy* 15: 90–91, 1993.
2. **Ameziane N, Beillat T, Verpillat P, Chollet-Martin S, Aumont MC, Seknadji P, Lamotte M, Lebret D, Ollivier V, and de Prost D.** Association of the toll-like receptor 4 gene Asp299Gly polymorphism with acute coronary events. *Arterioscler Thromb Vasc Biol* 23: e61–e64, 2003.
3. **Bjorklund M, Ciftcioglu N, and Kajander EO.** Extraordinary survival of nanobacteria under extreme conditions. *SPIE* 3441: 123–129, 1998.
4. **Blacher J, Guerin AP, Pannier B, Marchais SJ, and London GM.** Arterial calcifications, arterial stiffness, and cardiovascular risk in end-stage renal disease. *Hypertension* 38: 938–942, 2001.
5. **Boyan BD, Schwartz Z, Swain LD, Carnes DL Jr, and Zislis T.** Differential expression of phenotype by resting zone and growth region costochondral chondrocytes in vitro. *Bone* 9: 185–194, 1988.
6. **Boyan BD, Schwartz ZVI, Carnes DL Jr, and Ramirez V.** The effects of vitamin D metabolites on the plasma and matrix vesicle membranes of growth and resting cartilage cells in vitro. *Endocrinology* 122: 2851–2860, 1988.
7. **Burke AP, Tracy RP, Kolodgie F, Malcolm GT, Zieske A, Kutys R, Pestaner J, Smialek J, and Virmani R.** Elevated C-reactive protein values and atherosclerosis in sudden coronary death. Association with different pathologies. *Circulation* 105: 2019–2023, 2002.
8. **Burnett MS, Gaydos CA, Madico GE, Glad SM, Paigen B, Quinn TC, and Epstein SE.** Atherosclerosis in apoE knockout mice infected with multiple pathogens. *J Infect Dis* 183: 226–231, 2001.
9. **Ciftcioglu N and Kajander EO.** Interaction of nanobacteria with cultured mammalian cells. *Pathophysiology* 4: 259–270, 1998.
10. **Ciftcioglu N, Miller-Hjelle MA, Hjelle JT, and Kajander EO.** Inhibition of nanobacteria by antimicrobial drugs as measured by a modified microdilution method. *Antimicrob Agents Chemother* 46: 2077–2086, 2002.
11. **Cisar JO, Xu DQ, Thompson J, Swaim W, Hu L, and Kopecko DJ.** An alternative interpretation of nanobacteria-induced biomineralization. *Proc Natl Acad Sci USA* 97: 11511–11515, 2000.
12. **Domingue GJ and Schlegel JU.** Novel bacterial structures in human blood: cultural isolation. *Infect Immun* 15: 621–627, 1977.
13. **Domingue GJ, Sr. and Woody HB.** Bacterial persistence and expression of disease. *Clin Microbiol Rev* 10: 320–344, 1997.
14. **Drancourt M, Jacomo V, Lepidi H, Lechevallier E, Grisoni V, Coulange C, Ragni E, Alasia C, Dussol B, Berland Y, and Raoult D.** Attempted isolation of *Nanobacterium* sp. microorganisms from upper urinary tract stones. *J Clin Microbiol* 41: 368–372, 2003.
15. **Engstrom G, Stavenow L, Hedblad B, Lind P, Tyden P, Janzon L, and Lindgarde F.** Inflammation-sensitive plasma proteins and incidence of myocardial infarction in men with low cardiovascular risk. *Arterioscler Thromb Vasc Biol* 23: 2247–2251, 2003.
16. **Epstein SE, Zhu J, Burnett MS, Zhou YF, Vercellotti GM, and Hajjar D.** Infection and atherosclerosis: potential roles of pathogen burden and molecular mimicry. *Arterioscler Thromb Vasc Biol* 20: 1417–1420, 2000.
17. **Espinola-Klein C, Rupprecht HJ, Blankenberg S, Bickel C, Kopp H, Rippin G, Victor A, Hafner G, Schlumberger W, and Meyer J.** Impact of infectious burden on extent and long-term prognosis of atherosclerosis. *Circulation* 105: 15–21, 2002.
18. **Folk RL.** Bacteria and nannobacteria revealed in hardgrounds, calcite cements, native sulfur, sulfide minerals, and travertines. *Geological Society of America Annual Meeting, Abstracts with Programs*, 1992, vol. 24, p. 104.
19. **Folk RL.** SEM imaging of bacteria and nannobacteria in carbonate sediments and rocks. *J Sed Petrol* 63: 990–999, 1993.
20. **Folk RL and Lynch FL.** Organic matter, putative nannobacteria and the formation of ovoids and hardgrounds. *Sedimentology* 48: 215–229, 2001.
21. **Folk RL and Lynch FL.** The possible role of nannobacteria (dwarf bacteria) in clay-mineral diagenesis and the importance of careful sample preparation in high-magnification SEM study. *J Sed Res* 67: 583–589, 1997.
22. **Gibbs RGJ, Carey N, and Davies AH.** Chlamydia pneumoniae and vascular disease. *Br J Surg* 85: 1191–1197, 1998.
23. **Greenland P, LaBree L, Azen SP, Doherty TM, and Detrano RC.** Coronary artery calcium score combined with Framingham score for risk prediction in asymptomatic individuals. *JAMA* 291: 210–215, 2004.
24. **Hjelle JT, Miller-Hjelle MA, Poxton IR, Kajander EO, Ciftcioglu N, Jones ML, Caughey RC, Brown R, Millikin PD, and Darras FS.** Endotoxin and nanobacteria in polycystic kidney disease. *Kidney Int* 57: 2360–2374, 2000.
25. **Hsu HHT and Camacho NP.** Isolation of calcifiable vesicles from human atherosclerotic aortas. *Atherosclerosis* 143: 353–362, 1999.
26. **Huber H, Hohn MJ, Rachel R, Fuchs T, Wimmer VC, and Stetter KO.** A new phylum of Archaea represented by a nanosized hyperthermophilic symbiont. *Nature* 417: 63–67, 2002.
27. **Jelic TM, Malas AM, Groves SS, Jin B, Mellen PF, Osborne G, Roque R, Rosencrance JG, and Chang HH.** Nanobacteria-caused mitral valve calciphylaxis in a man with diabetic renal failure. *South Med J* 97: 194–198, 2004.
28. **Kajander EO and Ciftcioglu N.** Nanobacteria: an alternative mechanism for pathogenic intra- and extracellular calcification and stone formation. *Proc Natl Acad Sci USA* 95: 8274–8279, 1998.
29. **Kajander EO, Kuronen I, Akerman KK, Pelttari A, and Ciftcioglu N.** Nanobacteria from blood, the smallest culturable autonomously replicating agent on Earth. *SPIE* 3111: 420–428, 1997.
30. **Kerr RA.** Requiem for life on Mars? Support for microbes fades. *Science* 282: 1398–1400, 1998.
31. **Kiechl S, Egger G, Mayr M, Wiedermann CJ, Bonora E, Oberhollenzer F, Muggeo M, Xu Q, Wick G, Poewe W, and Willeit J.** Chronic infections and the risk of carotid atherosclerosis. Prospective results from a large population study. *Circulation* 103: 1064–1070, 2001.
32. **Kiechl S, Lorenz E, Reindl M, Wiedermann CJ, Oberhollenzer F, Bonora E, Willeit J, and Schwartz DA.** Toll-like receptor 4 polymorphisms and atherogenesis. *N Engl J Med* 347: 185–192, 2002.
33. **Kim KM.** Calcification of matrix vesicles in human aortic valve and aortic media. *Fed Proc* 35: 156–162, 1976.
34. **Kim KM and Trump BF.** Amorphous calcium precipitations in human aortic valve. *Calcif Tissue Res* 18: 155–160, 1975.
35. **Kirkland BL, Lynch FL, Rahnis M, Folk RL, Molineux I, and McLean RJC.** Alternative origins for nannobacteria-like objects in calcite. *Geology* 27: 347–350, 1999.
36. **Kockx MA and Herman AG.** Apoptosis in atherosclerosis: beneficial or detrimental? *Cardiovasc Res* 45: 736–746, 2000.
37. **Kockx MM, Muhring J, Bortier H, De Meyer GRY, and Jacob W.** Biotin- or digoxigenin-conjugated nucleotides bind to matrix vesicles in atherosclerotic plaques. *Am J Pathol* 148: 1771–1777, 1996.
38. **Maniloff J.** Nannobacteria: size limits and evidence (Letter). *Science* 276: 1776–1777, 1997.
39. **Martin GR, Schiffmann E, Bladen HA, and Nylen M.** Chemical and morphological studies on the in vitro calcification of aorta. *J Cell Biol* 16: 243–252, 1963.
40. **Nealson KH.** Nannobacteria: size limits and evidence (Reply). *Science* 276: 1776–1777, 1997.
41. **Pohle K, Maffert R, Ropers D, Moshage W, Stilianakis N, Daniel WG, and Achenbach S.** Progression of aortic valve calcification: association with coronary atherosclerosis and cardiovascular risk factors. *Circulation* 104: 1927–1932, 2001.
42. **Prasad A, Zhu J, Halcox JPJ, Waclawiw MA, Epstein SE, and Quyyumi AA.** Predisposition to atherosclerosis by infections. Role of endothelial dysfunction. *Circulation* 106: 184–190, 2002.
43. **Rappe MS, Connon SA, Vergin KL, and Glovannoni SJ.** Cultivation of the ubiquitous SAR11 marine bacterioplankton clade. *Nature* 418: 630–633, 2002.

44. **Ross R and Glomset JA.** The pathogenesis of atherosclerosis. *N Engl J Med* 295: 420–425, 1976.
45. **Sedivy R and Battistutti WB.** Nanobacteria promote crystallization of psammoma bodies in ovarian cancer. *APMIS* 111: 951–954, 2003.
46. **Shioi A, Nishizawa Y, Jono S, Koyama H, Hosoi M, and Morii H.** β-Glycerophosphate accelerates calcification in cultured bovine vascular smooth muscle cells. *Arterioscler Thromb Vasc Biol* 15: 2003–2009, 1995.
47. **Tintut Y and Demer LL.** Recent advances in multifactorial regulation of vascular calcification. *Curr Opin Lipidol* 12: 555–560, 2001.
48. **Tintut Y, Parhami F, Bostrom K, Jackson SM, and Demer LL.** cAMP stimulates osteoblast-like differentiation of calcifying vascular cells. Potential signaling pathway for vascular calcification. *J Biol Chem* 273: 7547–7553, 1998.
49. **Uwins PJR, Webb RI, and Taylor AP.** Novel nano-organisms from Australian sandstones. *Am Mineral* 83: 1541–1550, 1998.
50. **Vali H, McKee MD, Cifticioglu N, Sears K, Plows FL, Chevet E, Ghiabi P, Plavsic M, Kajander EO, and Zare RN.** Nanoforms: a new type of protein-associated mineralization. *Geochimica et Cosmochimica Acta* 65: 63–74, 2001.
51. **Vink A, Poppen J, Schoneveld AH, Roholl PJM, de Kleijn DPV, Borst C, and Pasterkamp G.** Distribution of *Chlamydia pneumoniae* in the human arterial system and its relation to the local amount of atherosclerosis within the individual. *Circulation* 103: 1613–1617, 2001.
52. **Wu LNY, Sauer GR, Genge BR, Valhmu WB, and Wuthier RE.** Effects of analogues of inorganic phosphate and sodium ion on mineralization of matrix vesicles isolated from growth plate cartilage of normal rapidly growing chickens. *J Inorg Biochem* 94: 221–235, 2003.